Strong coupling electron-photon dynamics: A real-time investigation of energy redistribution in molecular polaritons

Matteo Castagnola and Marcus T. Lexander
Department of Chemistry, Norwegian University of Science and Technology, 7491 Trondheim, Norway

Enrico Ronca*
Dipartimento di Chimica, Biologia e Biotecnologie, Università degli Studi di Perugia, Via Elce di Sotto 8, 06123 Perugia, Italy

Henrik Koch†
Department of Chemistry, Norwegian University of Science and Technology, 7491 Trondheim, Norway

(Received 24 April 2024; accepted 2 August 2024; published 11 September 2024)

We analyze the real-time electron-photon dynamics in long- and short-range energy transfer using a real-time quantum electrodynamics coupled cluster model, which allows for spatial and temporal visualization of transport processes. We compute the time evolution of photonic and molecular observables, such as the dipole moment and the photon coordinate, following the excitation of the system induced by short laser pulses. Our simulations show that intermolecular interactions and light-matter strong coupling lead to modified electronic polarization compared to the undressed molecules. The developed method can simulate multiple high-intensity laser pulses while explicitly retaining electronic and electron-photon correlation and is thus suited for nonlinear optics and transient absorption spectroscopies of molecular polaritons.

DOI: 10.1103/PhysRevResearch.6.033283

I. INTRODUCTION

When a molecular excitation strongly interacts with a confined optical mode (e.g., in a Fabry-Pérot cavity), hybrid light-matter states, called polaritons, are formed. Polaritons have recently attracted interest from chemists due to pioneering experiments proving modifications in chemical properties, such as photochemistry and ground-state reactivity [1–9]. Several works have suggested a modified electronic dynamics under light-matter strong coupling, showing, e.g., changes in lifetimes [1,10], selection rules in multiphoton absorption [11], and energy transfer [12–18], as well as enhanced nonlinear optical properties [19–23]. The proper understanding of such experimental findings in cavity-modified chemistry requires a microscopic model of the electron-photon interplay. To this end, theoretical methods that merge quantum optic models and theoretical chemistry have been proposed in recent years. *Ab initio* quantum electrodynamical methods, such as quantum electrodynamics coupled cluster [24] (QED-CC) and quantum electrodynamics density functional theory (QEDFT) [25–27], are based on electronic structure theory [28,29] to provide a nonperturbative description of the light-matter interaction, though, in general, limited to few molecules due to the computational costs. Other approaches treat the electronic degrees of freedom and the light-matter interaction at a lower level of theory but focus on the collective nature of polaritons starting, e.g., from Tavis-Cummings-like [30] models with parameters obtained from electronic structure calculations [31–33].

In this paper, we take another step forward in the *ab initio* description of molecular polaritons by explicitly modeling laser-driven molecules in quantum cavities. We present the first development and implementation of the real-time quantum electrodynamics coupled cluster method (RT-QED-CC). Real-time electronic structure methods have made significant progress [34] and, recently, some have been extended to molecular polaritons such as real-time (RT) quantum electrodynamics configuration interaction [35,36], real-time QEDFT [22,37–39], as well as semiclassical methods with a self-consistent coupling between the molecule and classical cavity modes [40]. Coupled cluster methodologies are very successful, both for the ground and the excited states [28], and their real-time implementations are suited for the electronic dynamics under strong and ultrashort laser pulses [41–46]. The *ab initio* QED-CC parametrization of the polaritonic wave function, which includes electron-electron and electron-photon correlation [24,28], provides a nonperturbative description of the electron-photon dynamics. We can hence reliably describe both the long-range photonic correlation and the short-range intra- and intermolecular electronic forces. The RT-QED-CC method is therefore suited for studying the interaction of molecules and aggregates with confined optical modes from the weak to the ultrastrong coupling

*Contact author: enrico.ronca@unipg.it
†Contact author: henrik.koch@ntnu.no

regime, even under external high-intensity and ultrashort electric pulses (linear and nonlinear excitation regimes). Our method can support the study of quantum light spectroscopies [47–53], high-order harmonic generation [19–21], and multiphoton and transient (pump-probe) spectroscopy of molecular polaritons [10,11,54,55]. As a case study, we here focus on photon-mediated energy transfer as a clear example of experimentally [12–16] and theoretically [17,56,57] investigated electron-photon dynamics with potential applications in light-harvesting systems.

Our method allows spatial and temporal visualization of the transport process, following nonperturbatively the photon dynamics and the electronic density displacement, giving us access to molecular observables such as the molecular multipoles. Moreover, the *ab initio* QED-CC wave function includes electron-photon correlation [24], and we thus describe nonperturbatively the effect of the molecule on photonic quantities such as the photon coordinate, without resorting to a few-level or perturbative description of the system. Our results highlight different timescales in the electron-photon dynamics, the role of dark states, and the modified interaction of polaritons with external pulses. Moreover, RT-QED-CC can also nonperturbatively model the short-range electronic energy transfer (Förster and Dexter), offering a clear discussion of the similarities and differences with the photonic channel. We find that when both light-matter strong coupling and intermolecular forces are relevant, the local electronic dynamics is further complicated and does not resemble the purely electronic or photonic process. Our results thus support the recent hypothesis that electronic properties can be modified from the interplay of light-matter strong coupling and local intermolecular interactions [58,59]. While our method is so far designed for electronic strong coupling (ESC), we believe the concepts we developed for energy redistribution can also be applied to vibrational strong coupling (VSC) [18,60–62], and the method could be extended to include nuclear motion [63].

The paper is organized as follows. First, we briefly introduce the theory behind *ab initio* quantum electrodynamics (QED) and describe the QED Hartree-Fock (QED-HF) and QED-CC methods. Next, we provide a detailed description of the real-time QED-CC wave function and discuss the information we can extract by explicitly modeling the photonic degrees of freedom. We then apply the RT-QED-CC method to study energy transfers in molecular polaritons. Finally, we summarize the main results presented in the paper and discuss future perspectives and applications of the developed framework.

II. *AB INITIO* COUPLED CLUSTER FOR MOLECULAR POLARITONS

In this section, we introduce the QED-HF and QED-CC methods and focus on the real-time description of the QED-CC parametrization. The photons are described at the same level as the electrons in a polaritonic wave function. To this end, we employ the nonrelativistic Pauli-Fierz Hamiltonian in the dipole approximation, Born-Oppenheimer approximation, and length representation [64,65], here expressed in second quantization and atomic units

$$\begin{aligned} H = &\sum_{pq} h_{pq} E_{pq} + \frac{1}{2}\sum_{pqrs} g_{pqrs} e_{pqrs} + h_{\mathrm{nuc}} \\ &+ \sqrt{\frac{\omega}{2}}\sum_{pq} (\boldsymbol{\lambda}\cdot\boldsymbol{d})_{pq} E_{pq} (b^\dagger + b) \\ &+ \frac{1}{2}\sum_{pqrs} (\boldsymbol{\lambda}\cdot\boldsymbol{d})_{pq} (\boldsymbol{\lambda}\cdot\boldsymbol{d})_{rs} E_{pq} E_{rs} + \omega b^\dagger b, \end{aligned} \tag{1}$$

where $E_{pq} = \sum_\sigma a^\dagger_{p\sigma} a_{q\sigma}$ and $e_{pqrs} = E_{pq}E_{rs} - \delta_{qr}E_{ps}$ are the spin-adapted singlet electronic operators in second quantization, where the indices p, q, r, and s label the one-electron basis [28]. The quantities h_{pq}, g_{pqrs}, and $\boldsymbol{d}_{pq}$ are the one-electron, two-electron, and dipole integrals, respectively. The operators $b^\dagger$ and b create and annihilate photons of a single effective photon mode of frequency ω. Finally, $\boldsymbol{\lambda} = \lambda\boldsymbol{\epsilon}$ is the light-matter coupling strength of the photon field along its polarization $\boldsymbol{\epsilon}$. The coupling λ is connected to the field quantization volume V_c,

$$\lambda = \sqrt{\frac{4\pi}{V_c}}, \tag{2}$$

and increases with the electromagnetic confinement in optic devices. It is thus treated as an external parameter to be set in the Hamiltonian. The first term in Eq. (1) is the electronic Hamiltonian routinely employed in quantum chemistry [28], the second term is the bilinear light-matter interaction, and the last term describes the energy of the photon field, while the third line is the dipole self-energy, which originates from the transformation from the velocity to the length form of the Hamiltonian and ensures numerical stability [64,66–68]. The Hamiltonian in Eq. (1) is employed for the *ab initio* QED-HF and QED-CC methods [24], which we briefly describe in the following sections.

A. QED-HF

The QED-HF wave function $|\mathrm{R}\rangle$ is the direct product of a Slater determinant $|\mathrm{HF}\rangle$ and a photonic state, in the following expressed as a linear combination of the states $(b^\dagger)^n|0\rangle$ with coefficients c_n:

$$|\mathrm{R}\rangle = |\mathrm{HF}\rangle \otimes \sum_n (b^\dagger)^n |0\rangle c_n, \tag{3}$$

where $|0\rangle$ is the photon vacuum. The optimal parameters are obtained from the variational principle by minimizing the expectation value of the Hamiltonian in Eq. (1) [24]. The orbitals are obtained by diagonalization of the QED-HF Fock matrix, while the photon state is a coherent state determined by the molecular dipole moment [24],

$$|\mathrm{R}\rangle = |\mathrm{HF}\rangle \otimes U_{\text{QED-HF}}|0\rangle \equiv U_{\text{QED-HF}}|\mathrm{HF}, 0\rangle, \tag{4}$$

where

$$U_{\text{QED-HF}} = \exp\left(- \frac{\boldsymbol{\lambda}\cdot\langle \mathrm{R}|\boldsymbol{d}|\mathrm{R}\rangle}{\sqrt{2\omega}} (b^\dagger - b)\right). \tag{5}$$

B. QED-CC

The QED-HF wave function of Eq. (4) provides the reference state of the QED-CC parametrization, and the coherent-state transformation is handled via a picture change of the Hamiltonian [24,65]. The QED-CC wave function is thus defined in the QED-HF coherent-state representation $\tilde{H} = U^{\dagger}_{\text{QED-HF}} H U_{\text{QED-HF}}$, that is, the Hamiltonian used to determine the CC amplitudes is transformed using Eq. (5):

$$\begin{aligned}\tilde{H} = &\sum_{pq} h_{pq} E_{pq} + \frac{1}{2}\sum_{pqrs} g_{pqrs} e_{pqrs} + h_{\text{nuc}} \\ &+ \sqrt{\frac{\omega}{2}}(\boldsymbol{\lambda}\cdot(\boldsymbol{d} - \langle \boldsymbol{d}\rangle_{\text{QED-HF}}))(b^{\dagger} + b) \\ &+ \frac{1}{2}(\boldsymbol{\lambda}\cdot(\boldsymbol{d} - \langle \boldsymbol{d}\rangle_{\text{QED-HF}}))^2 + \omega b^{\dagger} b. \end{aligned} \tag{6}$$

As for the electronic coupled cluster [28], the QED-CC wave function is given by an exponential parametrization

$$|\text{QED-CC}\rangle = e^{T}|\text{HF}, 0\rangle, \tag{7}$$

where the cluster operator T includes electronic, photonic, and electron-photon excitations [24]. In this paper, we use the QED-CCSD-1 model [24], which includes single and double excitations in the electronic space and a single excitation for the photon

$$T = T_e + T_{\text{int}} + T_p, \tag{8}$$

where

$$T_e = \sum_{ai} t_{ai} E_{ai} + \frac{1}{2}\sum_{aibj} t_{aibj} E_{ai} E_{bj}, \tag{9}$$

$$T_{\text{int}} = \sum_{ai} s_{ai} E_{ai} b^{\dagger} + \frac{1}{2}\sum_{aibj} s_{aibj} E_{ai} E_{bj} b^{\dagger}, \tag{10}$$

$$T_p = \gamma b^{\dagger}. \tag{11}$$

In these equations, i and j label occupied orbitals, and a and b label virtual orbitals of the QED-HF reference determinant. The operator T_e is the electronic cluster with singles t_{ai} and doubles t_{aibj} electronic excitation amplitudes [28], while T_p includes a single photonic amplitude γ and creates field excitations in the coherent-state representation [24,69]. Finally, T_{int} creates simultaneous excitations in the matter and photon manifold via the single-1-photon s_{ai} and double-1-photon s_{aibj} amplitudes. In the same way, the QED-CC dual state is defined as

$$\langle\Lambda| = \langle\text{HF}, 0| + \sum_{\mu,n} \bar{t}_{\mu n}\langle\mu, n|e^{-T}, \tag{12}$$

where $\bar{t}_{\mu n}$ are the Lagrangian multipliers for the $|\mu, n\rangle$ excitation [24,28]. The amplitudes and the multipliers are then obtained as in standard CC theory by projection of the Schrödinger equation.

The QED-CC parametrization allows for a flexible ground state description, including electron-electron and electron-photon correlation. Following the same approach as for electronic CC, we can then obtain information on the molecular-polariton excited states using the equation of motion or response formalism [24,28,65,70,71]. These effectively time-independent approaches rely upon the Fourier transformation of any perturbation applied to the system. In the following, we describe a different approach based on a real-time propagation of the CC amplitudes.

C. Real-time QED-CC

We aim to study the time evolution of the electron-photon system subject to an external field $V(t)$ such as an electric pump. The total Hamiltonian is thus $\tilde{H} + \tilde{V}(t)$ [in the QED-HF coherent state representation of Eq. (6)], and we parametrize the time evolution using time-dependent amplitudes $T(t)$ and a complex global-phase parameter $\alpha(t)$, similarly to electronic TD-CC [41–46]

$$|\text{QED-CC}\rangle(t) = e^{T(t)}|\text{HF}, 0\rangle e^{i\alpha(t)}. \tag{13}$$

The amplitudes are obtained by projection of the time-dependent Schrödinger equation [41,70,71]

$$\frac{d\alpha}{dt} = -\langle\text{HF}, 0|(\tilde{H} + \tilde{V}(t))e^{T(t)}|\text{HF}, 0\rangle, \tag{14}$$

$$\frac{dt_{\mu}}{dt} = -i\langle\mu, 0|e^{-T(t)}(\tilde{H} + \tilde{V}(t))e^{T(t)}|\text{HF}, 0\rangle, \tag{15}$$

$$\frac{d\gamma}{dt} = -i\langle\text{HF}, 1|e^{-T(t)}(\tilde{H} + \tilde{V}(t))e^{T(t)}|\text{HF}, 0\rangle, \tag{16}$$

$$\frac{ds_{\mu}}{dt} = -i\langle\mu, 1|e^{-T(t)}(\tilde{H} + \tilde{V}(t))e^{T(t)}|\text{HF}, 0\rangle, \tag{17}$$

and analogous equations hold for the QED-CC dual state (further details are provided in the Supplemental Material [72]).

While response theory would rely on a perturbative expansion to obtain linear and nonlinear response functions in the frequency domain [65,70,71], we numerically propagate the amplitudes and multipliers in time. We thus study the electron-photon dynamics computing the mean values of observables $\langle A\rangle$ at each time step:

$$\langle A\rangle(t) = \langle\Lambda(t)|A|\text{QED-CC}(t)\rangle. \tag{18}$$

The information in the frequency domain can then be obtained via a Fourier transform of Eq. (18). Notice that in QED, we have access to additional observables from the explicit modeling of the photon field compared to the standard electronic simulation. We can thus describe photon quantities such as the field coordinate $q = \frac{b+b^{\dagger}}{\sqrt{2\omega}}$, which is connected to the electric field of the photons in the cavity, or the number operator $N_{ph} = b^{\dagger}b$. We must then account for the picture change of the QED-HF coherent state transformation in Eq. (5) since the QED-CC wave function is defined for the Hamiltonian in Eq. (6) [65,73,74].

The RT-QED-CC approach allows for the description of the electron-photon dynamics under ultrashort and intense *classical* electric fields,

$$V(t) = \boldsymbol{d}\cdot\boldsymbol{E}_{\text{ext}}(t) = \boldsymbol{d}\cdot\boldsymbol{\mathcal{E}}_0(t)\,\cos(\omega_{\text{ext}}t + \varphi), \tag{19}$$

where $\mathcal{E}_0(t)$ is an envelope function that describes the shape of the external pulse, and the field-molecule interaction is in the length gauge and dipole approximation. Moreover, the explicit modeling of the photon field provides additional flexibility in the operator $V(t)$. Since we retain the photonic degrees of freedom explicitly, the description of the external light source is not limited, in principle, to the semiclassical expression in

Eq. (19). This would require a multimode description of the field in the Hamiltonian in Eq. (1) and the wave function, and we could then prepare and propagate the system, e.g., in the electronic ground state superimposed with a proper photon wave packet. Nevertheless, unless very few-photons or nonclassical light is employed, the classical and nonclassical description of the pump should give similar results, so in this paper we focus on the classical interaction term of Eq. (19). In addition, while standard molecular spectroscopy focuses on the molecular degrees of freedom, in a QED framework, we can also study the effect of perturbations that couple directly to the photon field (for instance, via external currents), such as

$$V(t) = \mathcal{A}_0(b + b^\dagger), \tag{20}$$

$$V(t) = i\mathcal{B}_0(b - b^\dagger), \tag{21}$$

and subsequently follow the evolution of molecular observables.

The RT-QED-CC method thus allows for a nonperturbative coherent and correlated time-dependent description of the interaction of photons and molecules, permitting the modeling of transient spectroscopies for molecular polaritons, quantum light spectroscopies, molecules in laser fields, and electron-photon entanglement [10,11,47,49,52,53,75].

III. RESULTS AND DISCUSSIONS

In this section, the RT-QED-CCSD-1 method is employed to study photon-mediated energy transfers. The RT-QED-CCSD-1 equations have been implemented in a private branch of the $e^{\mathcal{T}}$ program [76], and the computational and implementation details are provided in the Supplemental Material.

A. Intermolecular energy transfer

Electronic intermolecular energy transfer has been experimentally [12–16] and theoretically [17,56,57,60,77] investigated due to its potential applications in technologies, e.g., solar cells and light-harvesting systems. The theoretical simulation of such processes has been performed with simplified methods [17] and collective Tavis-Cummings-like approaches [56,57]. We here provide an *ab initio* QED-CC simulation in the time domain.

As a simple system to study the long-range polaritonic energy transfer, we consider two identical but perpendicular H_2 molecules in the xy plane, with the cavity field tuned to their first bright molecular excitation (see Fig. 1). The light-matter coupling strength is here set to $\lambda = 0.01$ a.u. with polarization $\boldsymbol{\epsilon} = (1/\sqrt{2}, 1/\sqrt{2}, 0)$, such that both the H_2 are coupled to the optical environment. The intermolecular distance is large enough to suppress any electronic coupling between them ($D = 50$ Å). The molecular geometries and further computational details are provided in the Supplemental Material. In Fig. 1, we show selected snapshots of the differential electronic density (compared to the ground state) in the xy plane following the interaction with an ultrashort classical electric pulse [see Eq. (19)] centered at $t = 20$ a.u. and polarized along the x direction (parallel to one of the H_2).[1] The densities are computed at each time step of the simulation from the CC density matrix

$$D_{pq} = \langle \Lambda(t)|E_{pq}|\text{QED-CC}(t)\rangle, \tag{22}$$

where p and q label the one-electron molecular orbitals, and it is visualized on a grid. While the electric field polarizes both molecules (see the second panel of Fig. 1), only one of them is excited after the pulse has passed because of their orientation. In the absence of the photon coupling, the electron density of the excited molecule oscillates in time while nothing would happen to the second H_2. However, when the system is coherently coupled to an optical environment such as a Fabry-Pérot cavity, the excited molecule can transfer energy to the photon field, which, in turn, excites the other H_2 molecule. In Fig. 1, we thus visualize the ultralong energy transfer mediated by the cavity field. For computational reasons, we used a specific orientation to selectively excite only one H_2. However, longer pulses can be used to selectively excite a single species and thus trigger a cavity-mediated energy transfer between different molecules in quantum cavities [12–16]. Notice that since no decoherence or decay is introduced in the simulation, the excitation will be transferred back and forth between the H_2 molecules in a quasiperiodic fashion. The photon losses, as well as the radiative and nonradiative decays of the molecular excitations, affect the dynamics, and they could be modeled phenomenologically, e.g., adding an anti-Hermitian term in the Hamiltonian [79], or using a multimode description of the photon field [80].

The electron-photon dynamics is more easily analyzed by studying the time evolution of observables such as the dipole moment $\boldsymbol{d}$ and the photon coordinate $q = (b^\dagger + b)/\sqrt{2\omega}$. In the upper panel of Fig. 2, we plot the x and y components of the dipole moment for the process pictorially illustrated in Fig. 1. The y component of the dipole moment provides a simple measure of the excitation of the second H_2. The panel illustrates the fast density fluctuations, while their envelope shows the slower energy transfer between the molecules. The time evolution of the dipole moment for the undressed (out-of-cavity) electron dynamics is reported in the Supplemental Material, and does not show any energy transfer due to the large distance between the molecules. To follow the excitation of the quantum cavity, we report the photon coordinate $\langle q\rangle = \langle b^\dagger + b\rangle/\sqrt{2\omega}$ in the lower panel of Fig. 2. Photon and matter observables show out-of-phase oscillations and seem to display a different time period, with two maxima for $\langle q\rangle$ in a single (back-and-forth) energy transfer between the H_2 molecules. The reason for this (apparent) period difference is that each $\langle q\rangle$ maximum refers to one of the H_2 transferring their excitation to the photon field. This is illustrated more clearly using two slightly different molecules, stretching the bond length of the H_2 along y. The dipole moment components and the photon coordinate for this system are illustrated in Fig. 3. The photon and matter degrees of freedom now exhibit the same characteristic time, but there are still two maxima in the photon coordinate for the back-and-forth energy transfer. However, the two peaks are

[1] Videos of the energy-transfer dynamics are available in Ref. [78].

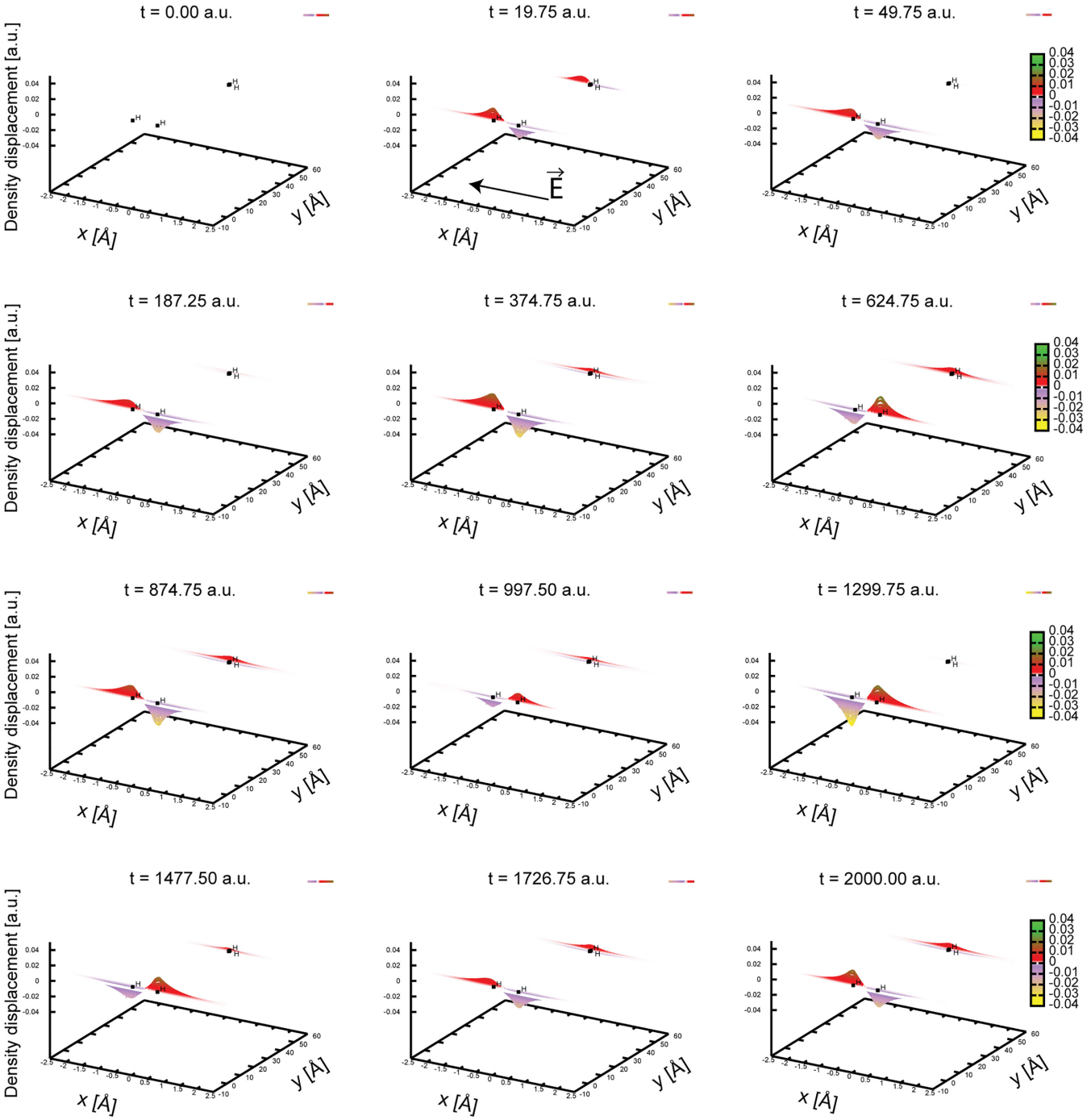

FIG. 1. Electron density displacement (compared to the molecular ground state) for two identical but perpendicular H_2 molecules placed on the xy plane at different times. The distance between them is $D = 50$ Å and the light-matter coupling strength is $\lambda = 0.01$ a.u., with photon polarization oriented such that both molecules are coupled to the cavity $\boldsymbol{\epsilon} = (1/\sqrt{2}, 1/\sqrt{2}, 0)$. The molecules are perturbed by an ultrashort classical electric pulse centered at 20 a.u. (second panel), but only the H_2 parallel to the classical electric field is excited after the pulse passes. The density of the excited molecule then oscillates in time. However, in a quantum cavity, the excitation is transferred to the photon field, which in turn excites the other H_2, thus allowing for ultralong range energy transfer. As time passes, the second molecule transfers its energy back to the photon field and eventually to the first molecule since no decoherence is present so far in the simulations.

now different as they refer to molecules with slightly different excitations transferring energy to the optical field. From Fig. 3, it is also clear that there are more timescales involved compared to Fig. 2, as can also be inferred from a simple Jaynes-Cummings (JC)-like analysis. The system in Fig. 1 is described as two identical two-level oscillators coupled to the cavity field. There are then three different eigenstates: the upper $|\mathrm{UP}\rangle$ and lower $|\mathrm{LP}\rangle$ polaritons, and one dark state $|\mathrm{DS}\rangle$ (of the same energy as the H_2 excited state and the photon)

$$|\mathrm{UP}\rangle = \frac{1}{\sqrt{2}}\left(\frac{|e_1 g_2 0\rangle + |g_1 e_2 0\rangle}{\sqrt{2}} + |g_1 g_2 1\rangle\right), \tag{23}$$

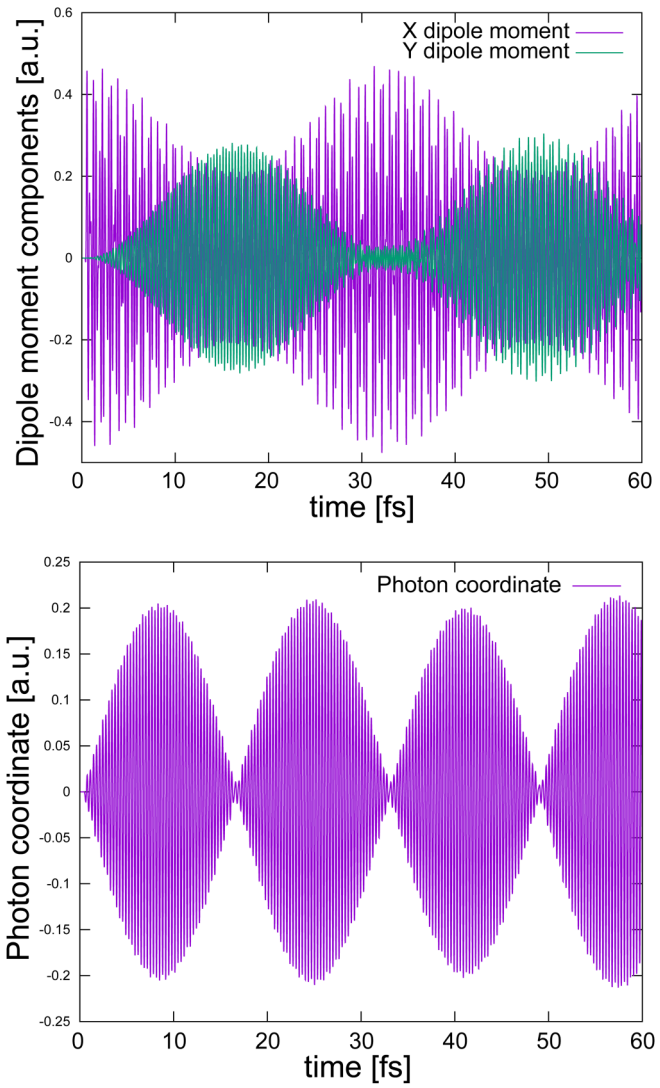

FIG. 2. Dipole moment $\boldsymbol{d}$ components (upper panel) and photon coordinate $\frac{\langle b^\dagger + b\rangle}{\sqrt{2\omega}}$ (lower panel) for the dynamics depicted in Fig. 1. The y component of the dipole moment provides a simple measure of the excitation transfer between the H_2 molecules, while the photon coordinate illustrates the photon excitation inside the cavity.

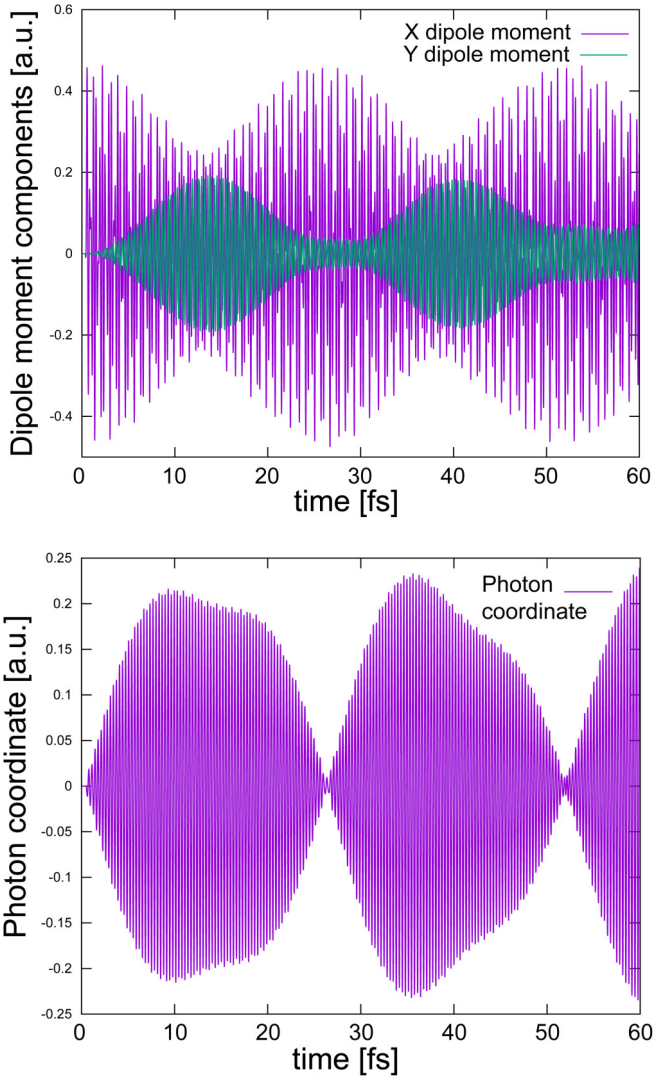

FIG. 3. Dipole moment $\boldsymbol{d}$ components (upper panel) and photon coordinate $\frac{\langle b^\dagger + b\rangle}{\sqrt{2\omega}}$ (lower panel) for the dynamics of two slightly different H_2 molecules (of bond lengths 0.76 Å and 0.78 Å), with orientation, cavity field, and external pulse as in Fig. 1. The system is thus endowed with three distinct polaritonic states (lower, middle, and upper polaritons). Since the two undressed H_2 excitations are slightly different, the maxima in the photon coordinate envelope (second panel) are now different, contrary to Fig. 2.

$$|\mathrm{DS}\rangle = \frac{|e_1 g_2 0\rangle - |g_1 e_2 0\rangle}{\sqrt{2}}, \tag{24}$$

$$|\mathrm{LP}\rangle = \frac{1}{\sqrt{2}}\left(\frac{|e_1 g_2 0\rangle + |g_1 e_2 0\rangle}{\sqrt{2}} - |g_1 g_2 1\rangle\right), \tag{25}$$

where e_p (g_p) refers to the pth H_2 molecule in the excited (ground) state, and 0 (1) to the zero- (one-) photon states. Note that the dark state $|\mathrm{DS}\rangle$, while showing no contribution from the photon field, has a nonzero transition dipole moment due to the different orientation of the molecules

$$\langle g_1 g_2 0|\boldsymbol{d}|DS\rangle = \frac{1}{\sqrt{2}}(\langle g_1|x_1|e_1\rangle, -\langle g_2|y_2|e_2\rangle, 0)^T. \tag{26}$$

After the pulse has passed, the system is still mainly in the ground state (linear excitation regime) superimposed with the polaritonic and dark states:

$$|e_1 g_2 0\rangle = \tfrac{1}{2}(|\mathrm{UP}\rangle + |\mathrm{LP}\rangle + \sqrt{2}|\mathrm{DS}\rangle). \tag{27}$$

The interference between the involved states thus generates the modulation of the oscillation amplitude (quantum beats) in Fig. 2. There are indeed three faster timescales associated with the excitation energies of the polaritonic and dark states, while there are two slower timescales in the envelope variation given by the Rabi splitting (UP-LP energy splitting) and the LP-DS energy difference. In fact, the LP-DS and UP-DS energy difference is the same and is exactly half the Rabi splitting. The role of the dark state is here to localize the wave function on one of the H_2. On the other hand, when the hydrogens are different, as in Fig. 3, three *polaritonic* states are formed: the UP, middle (MP), and LP polaritons. Using a JC-like model with parameters obtained from the

CCSD electronic structure simulations, we obtain a simple approximation for the polaritonic states:

$$|\mathrm{UP}\rangle \approx 0.60|e_1g_20\rangle + 0.31|g_1e_20\rangle + 0.74|g_1g_21\rangle, \quad (28)$$

$$|\mathrm{MP}\rangle \approx 0.75|e_1g_20\rangle - 0.55|g_1e_20\rangle - 0.37|g_1g_21\rangle, \quad (29)$$

$$|\mathrm{LP}\rangle \approx 0.29|e_1g_20\rangle + 0.77|g_1e_20\rangle - 0.56|g_1g_21\rangle. \quad (30)$$

Since the energies of $|e_1g_20\rangle$ and $|g_1e_20\rangle$ are different, all three states now show a different localization on the two molecules and a contribution from the photon field, and we have

$$|e_1g_20\rangle \approx 0.60|\mathrm{UP}\rangle + 0.29|\mathrm{LP}\rangle + 0.75|\mathrm{MP}\rangle. \quad (31)$$

In this case, three distinct timescales are present in the envelope variation (from the MP-LP, MP-UP, and LP-UP energy differences) [56], which explains why the photon revival in Fig. 3 differs from the first oscillation. In Figs. 2 and 3, we also see that the efficiency of the transfer changes. This can be understood from Eq. (31), where we see that the MP and UP contribute more than the LP in the initial state. The MP and LP are mainly localized on the $|e_1g_20\rangle$ state, while the LP has a larger contribution from the $|g_1e_20\rangle$ excitation, contrary to the identical-hydrogens setup where both states contribute the same to the eigenvectors [see Eqs. (28)–(30) and (23)–(25)]. The MP is known to be a fundamental state in the energy transfer process [16,56]. In the following, we discuss how the simultaneous effect of electronic and polaritonic pathways for energy transfer affects the molecular polarization.

Electronic energy transfer in chemistry usually arises from a dipole-dipole (Förster) or electronic-exchange (Dexter) mechanism, and both are highly dependent on the distance and orientation of the involved molecules [81]. Dexter energy transfer requires strong electronic couplings and is thus relevant only for very short distances, while the Förster mechanism decays as the sixth power of the intermolecular separation $1/R^6$. The Förster energy transfer also requires dipole-allowed molecular transitions and depends on the relative molecular orientation. On the other hand, the polaritonic mechanism is virtually distance independent, only requiring that both species show bright (dipole-allowed) molecular excitations coupled to a quasiresonant optical device [17,56,57]. Since the CC parametrization is size extensive and includes electron correlation, our method can reasonably describe intermolecular forces and is thus also suited for interacting molecules. We thus study the molecular dynamics when both the electronic and polaritonic energy transfer mechanisms are present simultaneously. In Fig. 4, we report the energy transfer between two H_2 molecules with the same parameters as in Fig. 1, but for a shorter intermolecular distance $D = 5$Å. The last panel of Fig. 4 shows the out-of-cavity (no QED) simulation of the x and y dipole moments, which illustrates the energy transfer due to the electronic coupling. The dynamics of the photon coordinate is very similar to the case of very distant hydrogens in Fig. 2. On the other hand, the dipole moment reported in the first panel of Fig. 4 shows that the molecular behavior is not as clean. While we recognize that both the electronic and polaritonic energy transfer mechanisms are involved, their interplay produces a dynamics which is different from both Fig. 2 and the out-of-cavity case in the

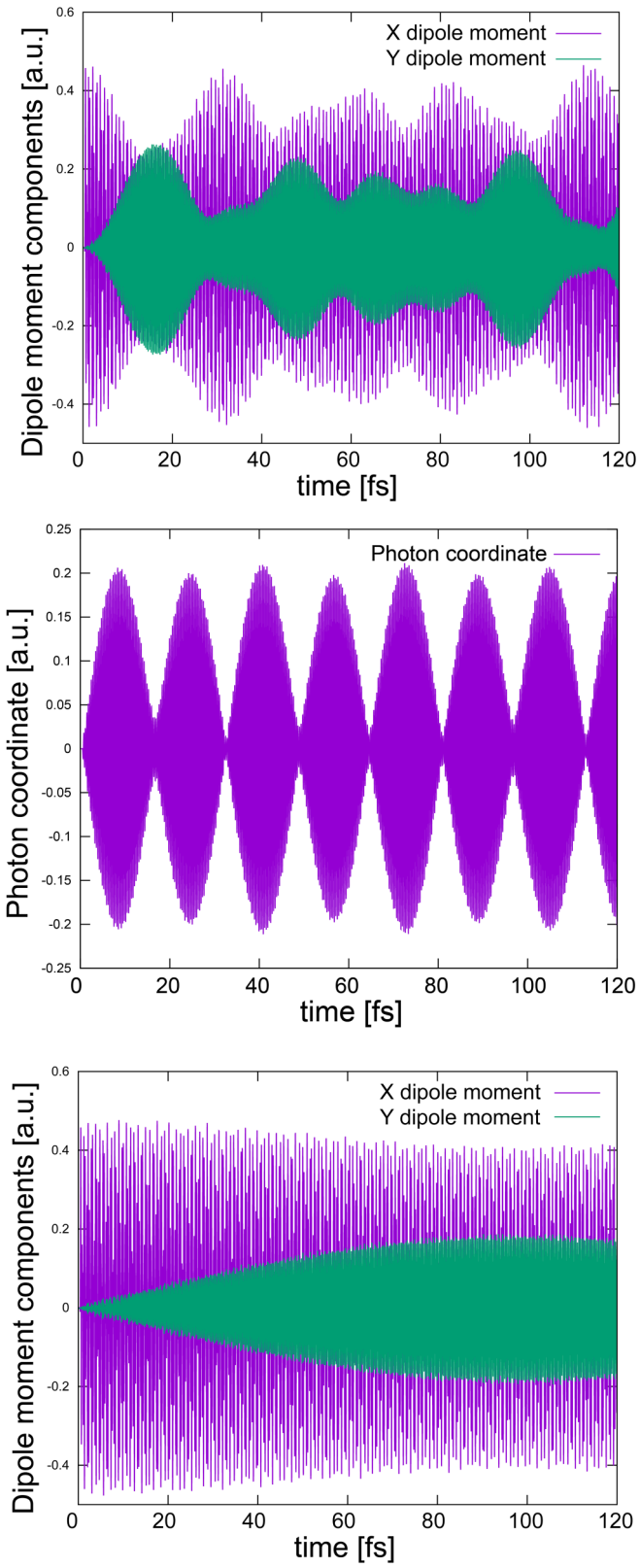

FIG. 4. Dipole moment $\boldsymbol{d}$ components (upper panel), photon coordinate $\frac{\langle b^\dagger + b\rangle}{\sqrt{2\omega}}$ (middle panel), and reference dipole moment simulation (no QED, lower panel) for the dynamics of two perpendicular but identical H_2 molecules at a distance of 5 Å. Due to electronic coupling, there is an energy transfer even in the absence of the photon field mediation.

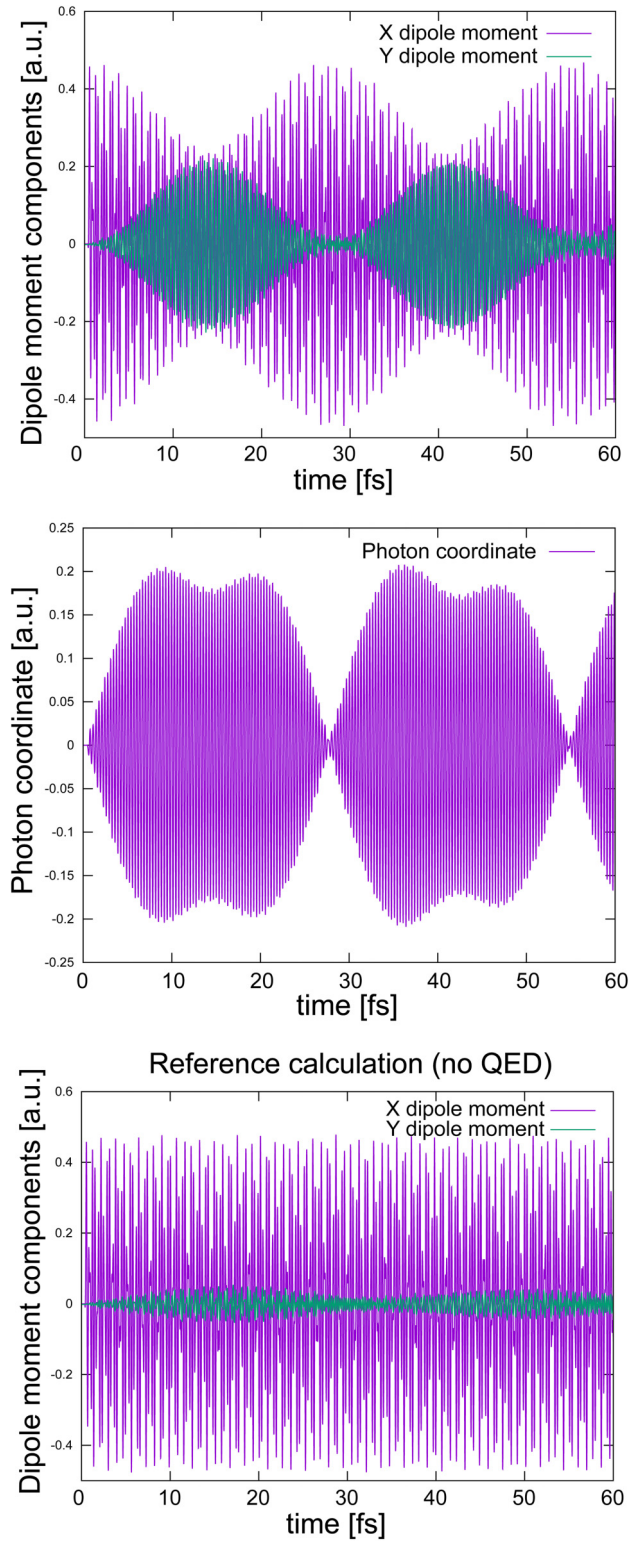

FIG. 5. Dipole moment $\boldsymbol{d}$ components (upper panel), photon coordinate $\frac{\langle b^\dagger + b\rangle}{\sqrt{2\omega}}$ (middle panel), and reference dipole moment simulation (no QED, lower panel) for the dynamics of two perpendicular H_2 molecules with a slightly different bond length at a distance of 5 Å. The electronic coupling is highly dependent on the excitation energy, the orientation, and the distance between the molecules and, compared to Fig. 4, little energy exchange occurs without the photon mediation.

last panel of Fig. 4. In Fig. 5, we show the same simulation for two slightly different H_2 molecules. Due to the different excitation energies, almost no energy transfer occurs without the photon field involvement (last panel), while two distinct photon maxima are highlighted due to the coupling of the different H_2 molecules to the optical device, as in Fig. 3. In this case, the intermolecular forces play a less relevant role, as revealed from the out-of-cavity simulation, and the dynamics resembles the one in Fig. 3. Therefore, Figs. 4 and 5 show that when both the electronic and light-matter coupling are relevant, the microscopic response is altered compared to the case when only one of the two interactions is present. These results hint in the same direction as recent theoretical and experimental works [58,59,67] which suggested modified electronic properties from the interplay of intermolecular forces and light-matter strong coupling. While RT-QED-CC is designed for electronic strong coupling, we expect similar processes to occur in vibrational strong coupling. These changes in the electronic polarization might then contribute to some effects observed in polaritonic chemistry, such as crystallization and assembly [82–84], modified interactions in aggregates, and solutions [58,59].

Finally, we investigated how the electron-photon dynamics changes with the light-matter coupling strength λ and the number of identical replicas N of the system (see also the Supplemental Material). Since the timescale of the photon-mediated energy transfer depends on the Rabi splitting, it is inversely proportional to λ and the square root of N. That is, the timescale depends only on the inverse of the *collective* coupling strength $\lambda\sqrt{N}$, which means that such processes are relevant in the thermodynamic limit $N \to \infty$, $\lambda\sqrt{N} = \text{const}$ and the timescales can be reduced by simply increasing the molecular concentration in the optical device. This is shown in the Supplemental Material for the systems of Figs. 2 and 3 (identical and different H_2 molecules). At the same time, the energy absorbed and the dipole moment oscillation amplitudes scale linearly when increasing the number of replicas N subject to the same external pulse. This is physically reasonable and is correctly modeled via the size intensivity and extensivity of the CC parametrization for the electrons [28,85]. On the other hand, the oscillation amplitudes of the photon coordinate scales as $\sqrt{N}$. The amplitude of matter and photon observables thus scale differently with N, while both are fundamentally independent on λ.

B. Photon generation and modified electron-photon dynamics *via* classical pulse sequences

We now focus on the energy transfer and electron-photon dynamics induced by multiple classical electric pulses. In Fig. 6, we report the time evolution of the dipole moment and photon coordinate induced by two short classical electric pulses centered at 20 a.u. and 550 a.u. for the same system depicted in Fig. 1. The second pulse is switched on just before the maximum transfer between the two H_2 molecules, and the undressed (out-of-cavity) electronic dynamics is reported in the last panel for reference. Notice that no energy transfer occurs outside the cavity because of the large separation between the molecules, as can be inferred from the absence of the y component of the dipole moment in the lowest panel.

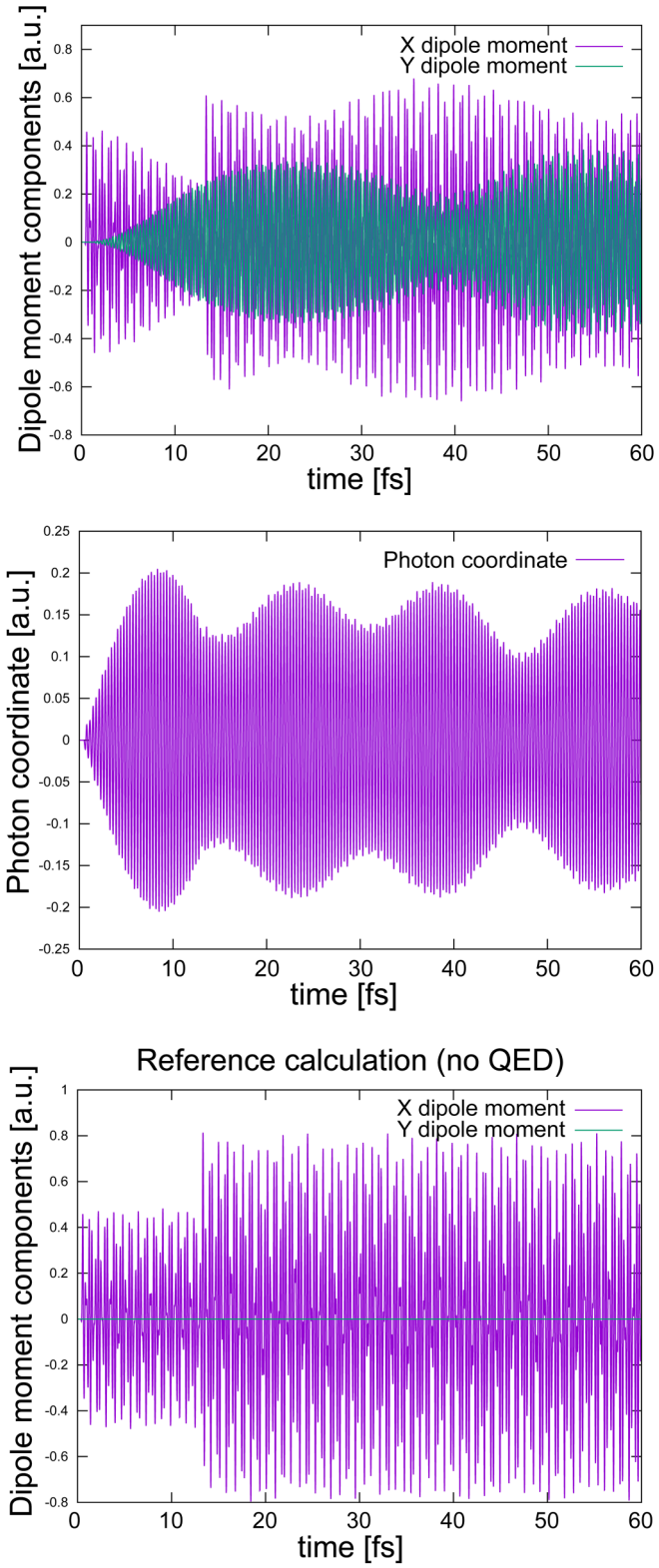

FIG. 6. Dipole moment $\boldsymbol{d}$ components (upper panel), photon coordinate $\frac{\langle b^\dagger + b\rangle}{\sqrt{2\omega}}$ (middle panel), and reference dipole moment simulation (no QED, lower panel) for the dynamics of two perpendicular but identical H_2 molecules at a distance of 50 Å. The system is excited via two ultrashort pulses centered at $t = 20$ a.u. and 550 a.u., where the second pulse is switched on just before the maximal energy transfer between the two H_2 molecules shown in Fig. 2.

TABLE I. Energy of the $(H_2)_2$ system before and after two ultrashort external electric pulses centered at $t = 20$ a.u. and 300 a.u.. For the undressed electrons, the molecule oriented along y does not participate in the simulation and the second pulse stimulates energy emission. In the QED simulation, after some energy has been transferred between the two H_2 molecules, the second pulse (slightly) excites the molecule along x again.

Energy (a.u.)	Initial	Pulse 1	Pulse 2
RT-QED-CC	−2.32991	−2.31173	−2.31083
RT-CC	−2.32998	−2.31180	−2.31296

The H_2 oriented along the external electric field (x axis) is excited again by the second pulse, causing a sharp change of the x component of the dipole moment. At the same time, the photon coordinate varies smoothly, but its envelope is modified compared to Fig. 2. Without the second pulse, the photon coordinate amplitude would decrease almost to zero, as shown in Fig. 2. After the H_2 along x is excited by the second pulse, the photon coordinate increases again, and its envelope amplitude never decreases to zero. This means that, through classical electric fields and their coupling only to matter, we generated photons in the optical device that the molecules will not completely absorb as in the vacuum Rabi oscillations of Fig. 2.

Another interesting point of the dynamics in Fig. 2 is the photon coordinate maximum, which occurs before the energy transfer between the H_2 is complete. In Fig. 7, we show the dynamics of the system under the influence of two pulses centered at 20 a.u. and 300 a.u.. The central time of the second pulse now roughly corresponds to the first maximum of $\langle q\rangle$ in Fig. 2. In Table I, we report the energy of the system (inside and outside the cavity) before and after each pulse. It is interesting that the optical device changes the interaction of the second pulse with the molecules. In the reference (no QED) simulation, the second pulse triggers a spontaneous emission as the system has lost energy after the interaction. Nevertheless, its effect is small enough that no sharp change in the dipole moment is shown in the last panel of Fig. 7. For the photon-dressed electrons, the molecules again gain energy from the pulse, as can be inferred from Table I. In this case, the dipole moment along x still does not show a sudden envelope modification, but there is a sharp change in the envelope of the photon coordinate. As in Fig. 6, the amplitude of the photon coordinate oscillations does not reduce to zero, contrary to Fig. 2, which means that there is always a nonzero number of photons inside the cavity. However, the photon coordinate amplitude is larger than Fig. 6, and the second H_2 molecule almost completely deexcites, contrary to the significant dipole moment along y shown in Fig. 6 after a complete oscillation. Thus, multiple classical pulses can trigger nontrivial photon dynamics in a quantum optic device and alter the photon-mediated energy transfer between molecules in the strong coupling regime. In particular, even though the interaction operator in Eq. (19) couples the external field only to the electronic degrees of freedom, shape changes can be obtained even in photonic quantities, as seen from the photon coordinate in Fig. 7.

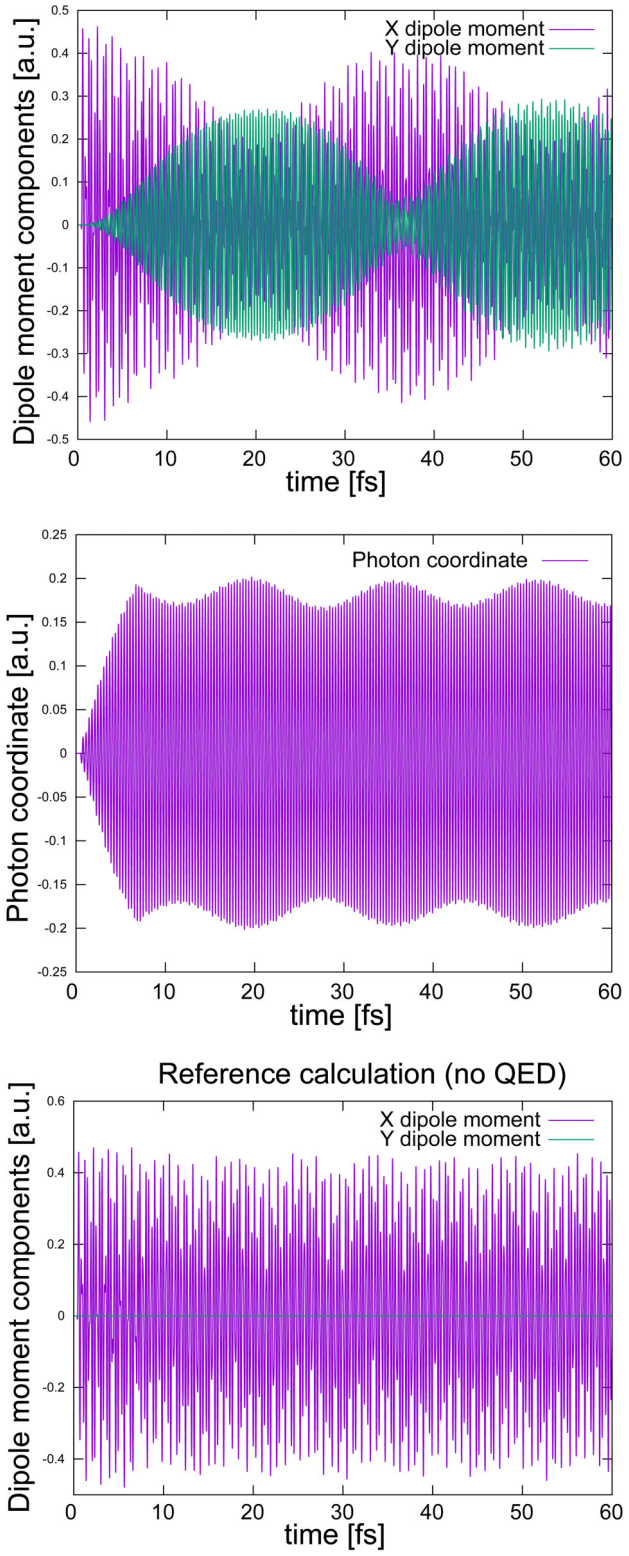

FIG. 7. Dipole moment $\boldsymbol{d}$ components (upper panel), photon coordinate $\frac{\langle b^\dagger + b\rangle}{\sqrt{2\omega}}$ (middle panel), and reference dipole moment simulation (no QED, lower panel) for the dynamics of two perpendicular but identical H_2 molecules at a distance of 50 Å. The system is excited via two ultrashort pulses centered at $t = 20$ a.u. and 300 a.u., where the second pulse is switched on roughly at the maximum amplitude of the photon coordinate q shown in Fig. 2.

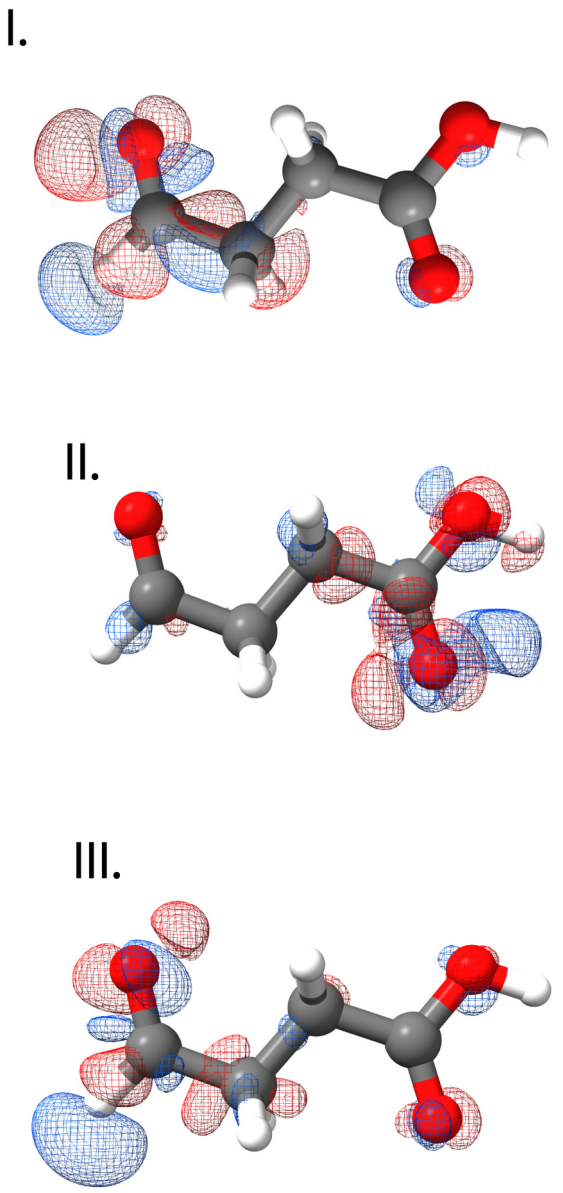

FIG. 8. Ground to excited state transition densities for three selected excited states of the succinic semialdehyde $C_4H_6O_3$. The colors indicate different signs in the transition density values. The excitation energies and the transition moments are reported in Table II. States I and III are mainly associated with the aldehyde moiety, while state II is an excitation of the acidic group.

C. Intramolecular electron-photon dynamics

While we have focused so far on intermolecular energy transfer, the described effects apply equally to intramolecular processes. As a chemically interesting system, we focus on the succinic semialdehyde $C_4H_6O_3$ illustrated in Fig. 8. In Fig. 8, we also report the transition density of three selected electronic excited states, whose excitation energy and dipole moments are reported in Table II (computational details and additional data can be found in the Supplemental Material). States I and III are primarily associated with the aldehyde moiety, while state II is an excitation of the acidic group. The molecule is then excited using a pulse centered at the energy of state II and polarized along x, thus coupling to

TABLE II. Excitation energies (eV) and product of the CCSD left and right transition dipole moments along x, y, and z $\langle L|d_p|CC\rangle\langle\Lambda|d_p|R\rangle$ (a.u.) for the excited states of the succinic semialdehyde $C_4H_6O_3$ depicted in Fig. 8.

State	Energy (eV)	x (a.u.)	y (a.u.)	z (a.u.)
I	7.144	0.0035	0.1041	0.0002
II	7.407	0.3813	0.0066	0.0000
III	7.802	0.1489	0.1681	0.0010

states II and III. For the QED simulation, the optical device is tuned to the undressed (out-of-cavity) excitation III reported in Table II, with moderate coupling strength $\lambda = 0.05$ a.u. and polarization along the xy axis. The photon field is thus coupled to all three reported states, while the other excitations of the molecule are less relevant as they are highly detuned and carry lower transition dipoles. The inspection of the density displacement after the interaction with the pulse shows that both the aldehyde and the acid group are excited. The acidic moiety shows a more significant density displacement (and thus excitation), as expected since the pulse carrier frequency is tuned to state II and from its larger transition moment along x (see also the Supplemental Material). In the first panel of Fig. 9, we report the time evolution of the x and y components of the dipole moments inside (solid lines) and outside (reference, dotted lines) the cavity. The results clearly show larger fluctuations for the y dipole moment in the QED environment compared to the noncavity case. States I and III are thus more involved in the polaritonic system than in the purely electronic dynamics. In addition, the absorbed energies (5.554×10^{-5} a.u. and 4.640×10^{-5} a.u. for the QED and reference electronic calculation, respectively) show a more favorable interaction of the external pulse with the polaritonic system. Therefore, the restructuring of the energy landscapes promoted by the light-matter strong coupling fundamentally changes the nature of the molecular excitation and can lead to more efficient interactions with external probes.

In the second panel of Fig. 9, we report the photon coordinate corresponding to different quantum pictures: the QED-HF coherent state representation, the length gauge, and the velocity gauge. That is, the computed quantities are

$$\frac{\langle b^\dagger + b\rangle}{\sqrt{2\omega}}(t), \tag{32}$$

$$\frac{\left\langle b^\dagger + b - \sqrt{\frac{2}{\omega}}\,\boldsymbol{\lambda}\cdot\langle\boldsymbol{d}\rangle_{\text{QED-HF}}\right\rangle}{\sqrt{2\omega}}(t), \tag{33}$$

$$\frac{\left\langle b^\dagger + b + \sqrt{\frac{2}{\omega}}\,\boldsymbol{\lambda}\cdot(\boldsymbol{d} - \langle\boldsymbol{d}\rangle_{\text{QED-HF}})\right\rangle}{\sqrt{2\omega}}(t), \tag{34}$$

where Eq. (33) corresponds to the operator $\frac{b^\dagger+b}{\sqrt{2\omega}}$ in the representation of Eqs. (1) and (34) to the same operator in the velocity gauge Hamiltonian [64–66,74]. These three quantities thus represent distinct observables. In particular, the photon coordinates of the velocity and length gauge describe the electric and displacement field operators, respectively [66,86]. While for the H_2 system, the differences in the computed values of these quantities are less relevant,

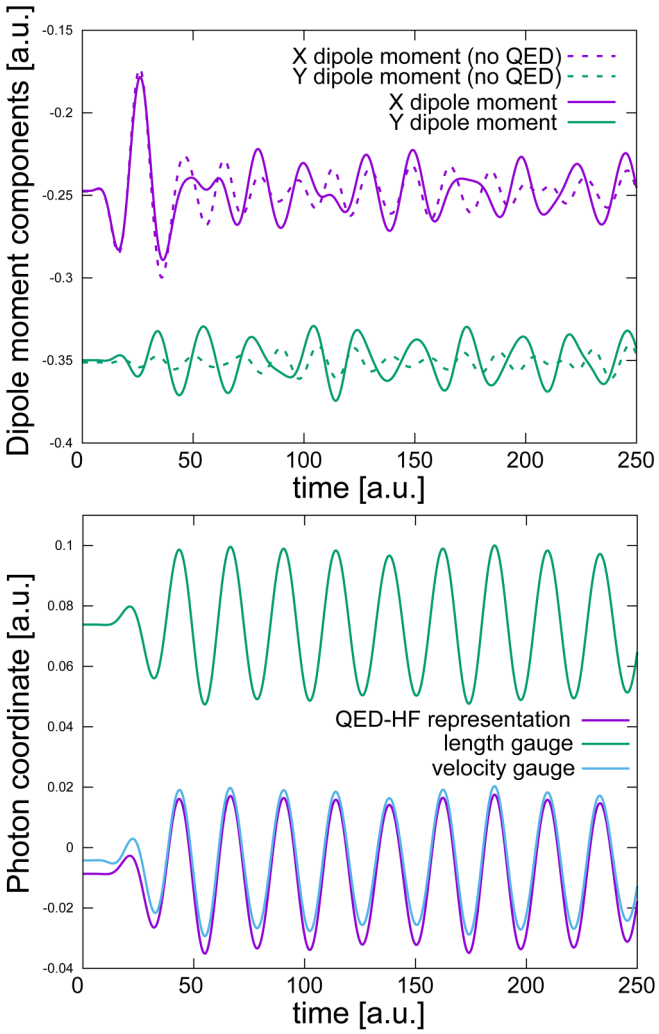

FIG. 9. Molecular (upper panel) and photon (lower panel) observables as a function of time for the succinic semialdehyde $C_4H_6O_3$. The cavity photon is resonant to state II of Table II and its polarization is along the xy axis, and thus coupled to all three states. Upper panel: Time evolution of the x and y components of the dipole moment inside (solid lines) and outside (reference, dotted lines) the cavity. The enhanced fluctuations (compared to the reference calculation) along y prove a larger cavity-induced energy transfer from state II to states II and III. Lower panel: Time evolution of the photon coordinate of different quantum pictures. The three reported quantities refer to different observables (the photon coordinate in the velocity and length gauge are proportional to the electric and displacement field operators, respectively), and the plot reminds us that care must be taken in identifying the correct mathematical expression for the physical observable of interest, as the results can change dramatically. We notice that the photon coordinate of the QED-HF coherent-state representation, although it does not have a clear physical significance, is similar to the photon coordinate of the velocity representation. This occurs because the permanent dipole of the molecule is already partially taken into account at the QED-HF level.

the permanent dipole moment of $C_4H_6O_3$ effectively shifts the photon coordinate values, as seen from Fig. 9. The fast oscillations of the photonic observables have an opposite sign of the oscillations in the y dipole moment, that is, they are de-

phased by π. Figure 9 thus numerically shows the importance of correctly identifying the mathematical operator describing physical observables. When reporting theoretical results, care must then be taken, specifying the Hamiltonian representation, the operator expression and its physical meaning since results can be very different and comparison between different simulations can lead to misunderstandings [65,66,73,74,86]. We also notice that, although the photon coordinate of the QED-HF representation in Eq. (32) does not correspond to any clear physical observable, its values provide a reasonable approximation of the velocity gauge photon coordinate during the whole simulation. This is a consequence of the coherent state transformation of Eq. (5), which partially accounts for the molecular dipole moment at the mean-field (HF) level of theory. Finally, we remark that, although different quantum pictures should be equivalent, numerical simulations performed in different representations will lead to different results due to the truncation of the matter and photon Hilbert spaces. From a molecular point of view, the length gauge is more convenient as the transition dipole moments decay rapidly with the energetic separation of the states, and thus good results can be obtained using truncated basis sets [74]. On the other hand, for extended systems such as solids, the velocity representation provides a more convenient formulation for the long wavelength approximation [87].

In addition, when the excited molecule transfers energy to the photon field, it can then be redistributed among all the states relevantly coupled to the optical device. The cavity field thus favors an energy redistribution from the acidic moiety to the aldehyde group (long-range energy transfer) via states I and III and vice versa. Notice, however, that these transfers of excitations are not equally feasible: state II has a larger transition dipole moment than I, and thus its coupling to the photon field is favored. The cavity also promotes an excitation rearrangement of the aldehyde, transferring energy from state II to state I. The intramolecular energy transfer between distant moieties of a large molecule is a chemically relevant potential application of electronic strong coupling. We thus speculate that electronic and vibrational strong coupling could affect charge migration and excitation transfer, which should be further investigated. In a sample with a large number of molecules, both inter- and intramolecular energy transfer would occur, and it might be challenging to separate the two effects. However, single-molecule (or few-molecule) light-matter strong coupling has been achieved in plasmonic cavities and the developed method and concepts apply equally to such devices.

IV. CONCLUSIONS

In this paper, we presented development and implementation of a real-time coupled cluster method with quantized electromagnetic fields (RT-QED-CC). Our model can describe the real-time electron-photon dynamics of molecules coupled to optic devices such as microcavities or plasmonic structures [88], providing the time evolution of both matter and photon observables. Moreover, the CC parametrization includes both electron-photon and short-range electron-electron correlation. The correlated *ab initio* description of light and matter can be used to simulate the QED dynamics under both intense external fields (linear and nonlinear excitation regimes) and considerable light-matter coupling strengths (weak to ultrastrong coupling). The method is also suited to describe the local intermolecular forces, which require a reliable description of the molecular density, and how they could be modified by their embedding in a structured optical environment, which is also suggested to induce local chemical effects [58,67,89].

We then applied the developed method to investigate the electron-photon dynamics of polariton-mediated energy transfer processes. Our method allows for a microscopic description of the electron-photon dynamics. The QED-CC wave function gives us access to the dipole moments and the photon coordinate, which provide a clear quantitative description of the system's evolution in the time domain. The spatial visualization of the transport process is also obtained from the computed molecular density. In addition, the CC wave function parametrization also allows for a quantitative description of electronic processes, such as Förster or Dexter energy transfer. We find that when both the polaritonic and electronic pathways are present in the system, the single-molecule dynamics is more involved. The electronic displacement is not a simple superposition of that of the two mechanisms. Our results then suggest that when both light-matter strong coupling and intermolecular forces play a relevant role, their interplay can fundamentally change the electronic properties, in agreement with some recent works [58,59,67]. Such local polarization changes can contribute to some of the chemical modifications observed in polaritonic chemistry [8,58,82]. We then show that energy exchange and electronic dynamics is also modified for intramolecular processes, providing a channel alternative to molecular vibrations. We thus speculate that experimental investigations of intramolecular charge and energy migration under electronic and vibrational strong coupling could provide unique applications of polaritonic chemistry. Finally, we show that multiple classical pulses can alter the energy transfer dynamics and generate nontrivial dynamics of real photons inside the optical device. While our method is focused on ESC, we believe the developed concepts are also valid for VSC [18,60–62].

The developed method is well-suited for supporting the study of experiments, including nonlinear optical processes [19–23], quantum-light [47–53], multiphoton, and transient absorption spectroscopies of molecules and molecular polaritons.[10,11,54,55] The study of nonlinear excitation regimes and pump-probe experiments in optical cavities will be investigated in future works, providing further insights into cavity-modified chemistry.

Videos of the energy transfer dynamics and output files are available in Ref. [78].

ACKNOWLEDGMENTS

M.C. acknowledges A.S. Skeidsvoll for insightful discussions. M.C. and H.K. acknowledge funding from the European Research Council (ERC) under the European Union's Horizon 2020 Research and Innovation Programme (Grant Agreement No. 101020016). M.L. and H.K. acknowledge funding from the Department of Chemistry at the Norwegian University of Science and Technology

(NTNU). E.R. acknowledges funding from the European Research Council (ERC) under the European Union's Horizon Europe Research and Innovation Programme (Grant No. ERC-StG-2021-101040197—QED-SPIN).

[1] J. A. Hutchison, T. Schwartz, C. Genet, E. Devaux, and T. W. Ebbesen, Modifying chemical landscapes by coupling to vacuum fields, Angew. Chem. Int. Ed. **51**, 1592 (2012).

[2] B. Munkhbat, M. Wersäll, D. G. Baranov, T. J. Antosiewicz, and T. Shegai, Suppression of photo-oxidation of organic chromophores by strong coupling to plasmonic nanoantennas, Sci. Adv. **4**, eaas9552 (2018).

[3] A. Thomas, J. George, A. Shalabney, M. Dryzhakov, S. J. Varma, J. Moran, T. Chervy, X. Zhong, E. Devaux, C. Genet *et al.*, Ground-state chemical reactivity under vibrational coupling to the vacuum electromagnetic field, Angew. Chem. **128**, 11634 (2016).

[4] J. Lather, P. Bhatt, A. Thomas, T. W. Ebbesen, and J. George, Cavity catalysis by cooperative vibrational strong coupling of reactant and solvent molecules, Angew. Chem. **131**, 10745 (2019).

[5] A. Thomas, L. Lethuillier-Karl, K. Nagarajan, R. M. Vergauwe, J. George, T. Chervy, A. Shalabney, E. Devaux, C. Genet, J. Moran *et al.*, Tilting a ground-state reactivity landscape by vibrational strong coupling, Science **363**, 615 (2019).

[6] A. Canaguier-Durand, E. Devaux, J. George, Y. Pang, J. A. Hutchison, T. Schwartz, C. Genet, N. Wilhelms, J.-M. Lehn, and T. W. Ebbesen, Thermodynamics of molecules strongly coupled to the vacuum field, Angew. Chem. Int. Ed. **52**, 10533 (2013).

[7] A. Sau, K. Nagarajan, B. Patrahau, L. Lethuillier-Karl, R. M. Vergauwe, A. Thomas, J. Moran, C. Genet, and T. W. Ebbesen, Modifying Woodward–Hoffmann stereoselectivity under vibrational strong coupling, Angew. Chem. Int. Ed. **60**, 5712 (2021).

[8] K. Hirai, R. Takeda, J. A. Hutchison, and H. Uji-i, Modulation of prins cyclization by vibrational strong coupling, Angew. Chem. **132**, 5370 (2020).

[9] W. Ahn, J. F. Triana, F. Recabal, F. Herrera, and B. S. Simpkins, Modification of ground-state chemical reactivity via light–matter coherence in infrared cavities, Science **380**, 1165 (2023).

[10] H. Wang, H.-Y. Wang, H.-B. Sun, A. Cerea, A. Toma, F. De Angelis, X. Jin, L. Razzari, D. Cojoc, D. Catone *et al.*, Dynamics of strongly coupled hybrid states by transient absorption spectroscopy, Adv. Funct. Mater. **28**, 1801761 (2018).

[11] K. Wang, W. Tao, K. Nagarajan, S. Kushida, K. Sandeep, C. Genet, and T. W. Ebbesen, Study of the selection rules of molecular polaritonic transitions by two-photon absorption spectroscopy, J. Phys. Chem. C **128**, 10534 (2024).

[12] K. Georgiou, R. Jayaprakash, A. Othonos, and D. G. Lidzey, Ultralong-range polariton-assisted energy transfer in organic microcavities, Angew. Chem. **133**, 16797 (2021).

[13] X. Zhong, T. Chervy, L. Zhang, A. Thomas, J. George, C. Genet, J. A. Hutchison, and T. W. Ebbesen, Energy transfer between spatially separated entangled molecules, Angew. Chem. **129**, 9162 (2017).

[14] X. Zhong, T. Chervy, S. Wang, J. George, A. Thomas, J. A. Hutchison, E. Devaux, C. Genet, and T. W. Ebbesen, Nonradiative energy transfer mediated by hybrid light-matter states, Angew. Chem. **128**, 6310 (2016).

[15] A. Cargioli, M. Lednev, L. Lavista, A. Camposeo, A. Sassella, D. Pisignano, A. Tredicucci, F. J. Garcia-Vidal, J. Feist, and L. Persano, Active control of polariton-enabled long-range energy transfer, Nanophotonics **13**, 2541 (2024).

[16] D. M. Coles, N. Somaschi, P. Michetti, C. Clark, P. G. Lagoudakis, P. G. Savvidis, and D. G. Lidzey, Polaritonmediated energy transfer between organic dyes in a strongly coupled optical microcavity, Nat. Mater. **13**, 712 (2014).

[17] C. Schäfer, M. Ruggenthaler, H. Appel, and A. Rubio, Modification of excitation and charge transfer in cavity quantum-electrodynamical chemistry, Proc. Natl. Acad. Sci. USA **116**, 4883 (2019).

[18] B. Xiang, R. F. Ribeiro, M. Du, L. Chen, Z. Yang, J. Wang, J. Yuen-Zhou, and W. Xiong, Intermolecular vibrational energy transfer enabled by microcavity strong light–matter coupling, Science **368**, 665 (2020).

[19] K. Wang, M. Seidel, K. Nagarajan, T. Chervy, C. Genet, and T. Ebbesen, Large optical nonlinearity enhancement under electronic strong coupling, Nat. Commun. **12**, 1486 (2021).

[20] F. Ge, X. Han, and J. Xu, Strongly coupled systems for nonlinear optics, Laser Photonics Rev. **15**, 2000514 (2021).

[21] T. Chervy, J. Xu, Y. Duan, C. Wang, L. Mager, M. Frerejean, J. A. Munninghoff, P. Tinnemans, J. A. Hutchison, C. Genet *et al.*, High-efficiency second-harmonic generation from hybrid light-matter states, Nano Lett. **16**, 7352 (2016).

[22] J. Malave, A. Ahrens, D. Pitagora, C. Covington, and K. Varga, Real-space, real-time approach to quantum–electrodynamical time-dependent density functional theory, J. Chem. Phys. **157**, 194106 (2022).

[23] B. Xiang, R. F. Ribeiro, Y. Li, A. D. Dunkelberger, B. B. Simpkins, J. Yuen-Zhou, and W. Xiong, Manipulating optical nonlinearities of molecular polaritons by delocalization, Sci. Adv. **5**, eaax5196 (2019).

[24] T. S. Haugland, E. Ronca, E. F. Kjønstad, A. Rubio, and H. Koch, Coupled cluster theory for molecular polaritons: Changing ground and excited states, Phys. Rev. X **10**, 041043 (2020).

[25] M. Ruggenthaler, J. Flick, C. Pellegrini, H. Appel, I. V. Tokatly, and A. Rubio, Quantum-electrodynamical density-functional theory: Bridging quantum optics and electronic-structure theory, Phys. Rev. A **90**, 012508 (2014).

[26] J. Flick, D. M. Welakuh, M. Ruggenthaler, H. Appel, and A. Rubio, Lightmatter response in nonrelativistic quantum electrodynamics, ACS Photonics **6**, 2757 (2019).

[27] I.-T. Lu, M. Ruggenthaler, N. Tancogne-Dejean, S. Latini, M. Penz, and A. Rubio, Electron-photon exchange-correlation approximation for QEDFT, arXiv:2402.09794.

[28] T. Helgaker, P. Jorgensen, and J. Olsen, *Molecular Electronic-Structure Theory* (John Wiley & Sons, Chichester, 2013).

[29] E. Engel, *Density Functional Theory* (Springer, Heidelberg, 2011).

[30] M. Tavis and F. W. Cummings, Exact solution for an *N*-molecule–radiation-field Hamiltonian, Phys. Rev. **170**, 379 (1968).

[31] H. L. Luk, J. Feist, J. J. Toppari, and G. Groenhof, Multiscale molecular dynamics simulations of polaritonic chemistry, J. Chem. Theory Comput. **13**, 4324 (2017).

[32] G. Groenhof, C. Climent, J. Feist, D. Morozov, and J. J. Toppari, Tracking polariton relaxation with multiscale molecular dynamics simulations, J. Phys. Chem. Lett. **10**, 5476 (2019).

[33] I. Sokolovskii, R. H. Tichauer, D. Morozov, J. Feist, and G. Groenhof, Multi-scale molecular dynamics simulations of enhanced energy transfer in organic molecules under strong coupling, Nat. Commun. **14**, 6613 (2023).

[34] X. Li, N. Govind, C. Isborn, A. E. DePrince III, and K. Lopata, Real-time time-dependent electronic structure theory, Chem. Rev. **120**, 9951 (2020).

[35] J. D. Weidman, M. S. Dadgar, Z. J. Stewart, B. G. Peyton, I. S. Ulusoy, and A. K. Wilson, Cavity-modified molecular dipole switching dynamics, J. Chem. Phys. **160**, 094111 (2024).

[36] B. G. Peyton, J. D. Weidman, and A. K. Wilson, Lightinduced electron dynamics of molecules in cavities: Comparison of model Hamiltonians, J. Opt. Soc. Am. B **41**, C74 (2024).

[37] J. J. Goings, P. J. Lestrange, and X. Li, Real-time timedependent electronic structure theory, Wiley Interdiscip. Rev.: Comput. Mol. Sci. **8**, e1341 (2018).

[38] T. Sato, H. Pathak, Y. Orimo, and K. L. Ishikawa, Communication: Time-dependent optimized coupled-cluster method for multielectron dynamics, J. Chem. Phys. **148**, 051101 (2018).

[39] R. Jestädt, M. Ruggenthaler, M. J. Oliveira, A. Rubio, and H. Appel, Light-matter interactions within the Ehrenfest–Maxwell–Pauli–Kohn–Sham framework: Fundamentals, implementation, and nano-optical applications, Adv. Phys. **68**, 225 (2019).

[40] T. E. Li, Z. Tao, and S. Hammes-Schiffer, Semiclassical real-time nuclear-electronic orbital dynamics for molecular polaritons: Unified theory of electronic and vibrational strong couplings, J. Chem. Theory Comput. **18**, 2774 (2022).

[41] B. S. Ofstad, E. Aurbakken, Ø. S. Schøyen, H. E. Kristiansen, S. Kvaal, and T. B. Pedersen, Time-dependent coupled-cluster theory, WIREs Comput. Mol. Sci. **13**, e1666 (2023).

[42] A. S. Skeidsvoll, A. Balbi, and H. Koch, Time-dependent coupled-cluster theory for ultrafast transient-absorption spectroscopy, Phys. Rev. A **102**, 023115 (2020).

[43] A. S. Skeidsvoll, T. Moitra, A. Balbi, A. C. Paul, S. Coriani, and H. Koch, Simulating weak-field attosecond processes with a Lanczos reduced basis approach to time-dependent equation-of-motion coupled-cluster theory, Phys. Rev. A **105**, 023103 (2022).

[44] D. R. Nascimento and A. E. DePrince, A general time-domain formulation of equation-of-motion coupledcluster theory for linear spectroscopy, J. Chem. Phys. **151**, 204107 (2019).

[45] T. B. Pedersen and S. Kvaal, Symplectic integration and physical interpretation of time-dependent coupled-cluster theory, J. Chem. Phys. **150**, 144106 (2019).

[46] C. Huber and T. Klamroth, Explicitly time-dependent coupled cluster singles doubles calculations of laser–driven many-electron dynamics, J. Chem. Phys. **134**, 054113 (2011).

[47] K. E. Dorfman, F. Schlawin, and S. Mukamel, Nonlinear optical signals and spectroscopy with quantum light, Rev. Mod. Phys. **88**, 045008 (2016).

[48] F. Schlawin and S. Mukamel, Two-photon spectroscopy of excitons with entangled photons, J. Chem. Phys. **139**, 244110 (2013).

[49] M. Ruggenthaler, N. Tancogne-Dejean, J. Flick, H. Appel, and A. Rubio, From a quantum-electrodynamical lightmatter description to novel spectroscopies, Nat. Rev. Chem. **2**, 0118 (2018).

[50] M. G. Raymer, T. Landes, and A. H. Marcus, Entangled two-photon absorption by atoms and molecules: A quantum optics tutorial, J. Chem. Phys. **155**, 081501 (2021).

[51] F. Schlawin, K. E. Dorfman, and S. Mukamel, Entangled two-photon absorption spectroscopy, Acc. Chem. Res. **51**, 2207 (2018).

[52] Y. L. A. Rezus, S. G. Walt, R. Lettow, A. Renn, G. Zumofen, S. Götzinger, and V. Sandoghdar, Single-photon spectroscopy of a single molecule, Phys. Rev. Lett. **108**, 093601 (2012).

[53] J.-M. Raimond, M. Brune, and S. Haroche, Manipulating quantum entanglement with atoms and photons in a cavity, Rev. Mod. Phys. **73**, 565 (2001).

[54] B. Gu, Y. Gu, V. Y. Chernyak, and S. Mukamel, Cavity control of molecular spectroscopy and photophysics, Acc. Chem. Res. **56**, 2753 (2023).

[55] C. A. DelPo, B. Kudisch, K. H. Park, S.-U.-Z. Khan, F. Fassioli, D. Fausti, B. P. Rand, and G. D. Scholes, Polariton transitions in femtosecond transient absorption studies of ultrastrong light-molecule coupling, J. Phys. Chem. Lett. **11**, 2667 (2020).

[56] R. Sáez-Blázquez, J. Feist, A. I. Fernández-Domínguez, and F. García-Vidal, Organic polaritons enable local vibrations to drive long-range energy transfer, Phys. Rev. B **97**, 241407(R) (2018).

[57] M. Du, L. A. Martínez-Martínez, R. F. Ribeiro, Z. Hu, V. M. Menon, and J. Yuen-Zhou, Theory for polaritonassisted remote energy transfer, Chem. Sci. **9**, 6659 (2018).

[58] S. Biswas, M. Mondal, G. Chandrasekharan, A. Singh, and A. Thomas, Electronic strong coupling modifies the ground-state intermolecular interactions in chlorin thin films, doi: 10.26434/chemrxiv-2024-14r7s.

[59] B. Patrahau, M. Piejko, R. J. Mayer, C. Antheaume, T. Sangchai, G. Ragazzon, A. Jayachandran, E. Devaux, C. Genet, J. Moran *et al.*, Direct observation of polaritonic chemistry by nuclear magnetic resonance spectroscopy, Angew. Chem. Int. Ed. **63**, e202401368 (2024).

[60] J. Cao, Generalized resonance energy transfer theory: Applications to vibrational energy flow in optical cavities, J. Phys. Chem. Lett. **13**, 10943 (2022).

[61] D. J. Tibben, G. O. Bonin, I. Cho, G. Lakhwani, J. Hutchison, and D. E. Gómez, Molecular energy transfer under the strong light–matter interaction regime, Chem. Rev. **123**, 8044 (2023).

[62] T. E. Li, A. Nitzan, and J. E. Subotnik, Collective vibrational strong coupling effects on molecular vibrational relaxation and energy transfer: Numerical insights via cavity molecular dynamics simulations, Angew. Chem. **133**, 15661 (2021).

[63] M. T. Lexander, S. Angelico, E. F. Kjønstad, and H. Koch, Analytical evaluation of ground state gradients in quantum electrodynamics coupled cluster theory, arXiv:2406.08107.

[64] M. Ruggenthaler, D. Sidler, and A. Rubio, Understanding polaritonic chemistry from *ab initio* quantum electrodynamics, Chem. Rev. **123**, 11191 (2023).

[65] M. Castagnola, R. R. Riso, A. Barlini, E. Ronca, and H. Koch, Polaritonic response theory for exact and approximate wave functions, WIREs Comput. Mol. Sci. **14**, e1684 (2024).

[66] C. Schäfer, M. Ruggenthaler, V. Rokaj, and A. Rubio, Relevance of the quadratic diamagnetic and selfpolarization terms

in cavity quantum electrodynamics, ACS Photonics **7**, 975 (2020).

[67] M. Castagnola, T. S. Haugland, E. Ronca, H. Koch, and C. Schäfer, Collective strong coupling modifies aggregation and solvation, J. Phys. Chem. Lett. **15**, 1428 (2024).

[68] V. Rokaj, D. M. Welakuh, M. Ruggenthaler, and A. Rubio, Light–matter interaction in the long-wavelength limit: no ground-state without dipole self-energy, J. Phys. B: At. Mol. Opt. Phys. **51**, 034005 (2018).

[69] M. D. Liebenthal, N. Vu, and A. E. DePrince III, Assessing the effects of orbital relaxation and the coherentstate transformation in quantum electrodynamics density functional and coupled-cluster theories, J. Phys. Chem. A **127**, 5264 (2023).

[70] T. B. Pedersen and H. Koch, Coupled cluster response functions revisited, J. Chem. Phys. **106**, 8059 (1997).

[71] H. Koch and P. Jorgensen, Coupled cluster response functions, J. Chem. Phys. **93**, 3333 (1990).

[72] See Supplemental Material at http://link.aps.org/supplemental/10.1103/PhysRevResearch.6.033283 for the computational details of all the calculations, details on the RT-QED-CCSD-1 implementation in $e^{\mathcal{T}}$, and additional simulations of the systems under study.

[73] J. J. Foley, J. F. McTague, and A. E. DePrince, *Ab initio* methods for polariton chemistry, Chem. Phys. Rev. **4**, 041301 (2023).

[74] A. Mandal, M. A. Taylor, B. M. Weight, E. R. Koessler, X. Li, and P. Huo, Theoretical advances in polariton chemistry and molecular cavity quantum electrodynamics, Chem. Rev. **123**, 9786 (2023).

[75] F. Schlawin, Entangled photon spectroscopy, J. Phys. B: At. Mol. Opt. Phys. **50**, 203001 (2017).

[76] S. D. Folkestad, E. F. Kjønstad, R. H. Myhre, J. H. Andersen, A. Balbi, S. Coriani, T. Giovannini, L. Goletto, T. S. Haugland, A. Hutcheson *et al.*, e^T 1.0: An open source electronic structure program with emphasis on coupled cluster and multilevel methods, J. Chem. Phys. **152**, 184103 (2020).

[77] G. Groenhof and J. J. Toppari, Coherent light harvesting through strong coupling to confined light, J. Phys. Chem. Lett. **9**, 4848 (2018).

[78] M. Castagnola, "Strong coupling electron-photon dynamics: A real-time investigation of energy redistribution in molecular polaritons", Zenodo (2024), doi: 10.5281/zenodo.10813660.

[79] C. Fábri, A. G. Császár, G. J. Halász, L. S. Cederbaum, and Á. Vibók, Coupling polyatomic molecules to lossy nanocavities: Lindblad vs schrodinger description, J. Chem. Phys. **160**, 214308 (2024).

[80] D. S. Wang, T. Neuman, J. Flick, and P. Narang, Light matter interaction of a molecule in a dissipative cavity from first principles, J. Chem. Phys. **154**, 104109 (2021).

[81] G. D. Scholes, Long-range resonance energy transfer in molecular systems, Annu. Rev. Phys. Chem. **54**, 57 (2003).

[82] K. Joseph, S. Kushida, E. Smarsly, D. Ihiawakrim, A. Thomas, G. L. Paravicini-Bagliani, K. Nagarajan, R. Vergauwe, E. Devaux, O. Ersen *et al.*, Supramolecular assembly of conjugated polymers under vibrational strong coupling, Angew. Chem. Int. Ed. **60**, 19665 (2021).

[83] K. Hirai, H. Ishikawa, T. Chervy, J. A. Hutchison, and H. Uji-i, Selective crystallization via vibrational strong coupling, Chem. Sci. **12**, 11986 (2021).

[84] K. Sandeep, K. Joseph, J. Gautier, K. Nagarajan, M. Sujith, K. G. Thomas, and T. W. Ebbesen, Manipulating the self-assembly of phenyleneethynylenes under vibrational strong coupling, J. Phys. Chem. Lett. **13**, 1209 (2022).

[85] A. S. Skeidsvoll and H. Koch, Comparing real-time coupled-cluster methods through simulation of collective Rabi oscillations, Phys. Rev. A **108**, 033116 (2023).

[86] C. Cohen-Tannoudji, J. Dupont-Roc, and G. Grynberg, *Photons and Atoms—Introduction to Euantum Electrodynamics* (J. Wiley, New York, 1997).

[87] M. K. Svendsen, M. Ruggenthaler, H. Hübener, C. Schäfer, M. Eckstein, A. Rubio, and S. Latini, Theory of quantum light-matter interaction in cavities: extended systems and the long wavelength approximation, arXiv:2312.17374.

[88] M. Romanelli, R. R. Riso, T. S. Haugland, E. Ronca, S. Corni, and H. Koch, Effective single-mode methodology for strongly coupled multimode molecular-plasmon nanosystems, Nano Lett. **23**, 4938 (2023).

[89] T. S. Haugland, C. Schäfer, E. Ronca, A. Rubio, and H. Koch, Intermolecular interactions in optical cavities: An *ab initio* QED study, J. Chem. Phys. **154**, 094113 (2021).